tvst

DOI: 10.1167/tvst.6.6.5

Article

Creating a Full-thickness Choroidal Incision: An Ex Vivo Analysis of Human and Porcine Tissue Contraction Dynamics

Stephen A. LoBue[1], Norihiro Yamada[1,2], Moon Jeong Choi[3], and Timothy W. Olsen[1,4]

[1] Emory University, Department of Ophthalmology, Atlanta GA, USA
[2] Gunma University, Department of Ophthalmology, Maebashi, Gunma Prefecture, Japan
[3] Kim's Eye Hospital, Seoul, South Korea
[4] Mayo Clinic, Department of Ophthalmology, Rochester, MN, USA

Correspondence: Timothy W. Olsen, Mayo Clinic, 200 First Street SW, Rochester, MN 55905 USA. e-mail: olsen.timothy@mayo.edu

Received: 12 July 2017
Accepted: 30 September 2017
Published: 7 November 2017

Keywords: choroid; surgery; incision; pig; porcine; contraction; elasticity; choroidal translocation; choroidal biopsy

Citation: LoBue SA, Yamada N, Choi MJ, Olsen TW. Creating a full-thickness choroidal incision: an ex vivo analysis of human and porcine tissue contraction dynamics. Trans Vis Sci Tech. 2017;6(6):5, doi: 10.1167/tvst.6.6.5

Purpose: We hypothesized that the elastic nature of the choroid leads to tissue contraction following a full-thickness, sharp incision. Furthermore, we sought to quantify, measure, and compare tissue contraction in ex vivo porcine globes and human globes of various ages using predetermined variables.

Method: A full-thickness, ex vivo choroidal incision was performed in either pig ($n = 97$) or human ($n = 30$) specimens. Variables included trephine diameter (1.5, 2.0, or 2.5 mm) versus a straight surgical blade, and temperature (1.7 °–4.4° vs. 36.6°F). Central centripetal and surround centrifugal tissue contractions were measured. Mean percentage tissue contraction was assessed as a ratio of trephine diameter to final tissue contraction measured immediately following each incision using a standardized device.

Results: For trephination in pig specimens, centripetal contraction ranged from 38% to 50% with a mean of 44%. Centrifugal contraction was approximately 15%. Human choroidal contraction was 39% and 15%, respectively, with a statistically significant inverse relationship to age ($R^2 = 0.35$, $P \leq 0.01$). Asymmetric contraction was noted when incisions were closer to choroidal attachment sites to the sclera, such as near vortex ampullae. Linear incisions resulted in contraction that correlated with incision length ($R^2 = 0.35$, $P \leq 0.001$).

Conclusions: A full-thickness choroidal incision results in significant tissue contraction. For circular incisions, the centripetal contraction approaches 50% of the original incision size. For linear incisions, the contraction corresponds directly with incision length. In human specimens, there is less contraction with advancing age.

Translational Relevance: Our findings have clinical relevance for choroidal biopsy, traumatic injury, and choroidal translocation surgery.

Introduction

The choroid contains a dense network of blood vessels that serve as the key vascular supply to the retinal pigment epithelium (RPE) and outer retina. Choroidal tissue is positioned between the RPE and sclera. The choroid has been determined to have the highest blood flow by weight of any tissue in the human body with the majority of the blood flow delivered to the posterior region.[1] Early physiologic studies by Alm and Bill[1] suggest that the choroidal blood flow, as measured as a ratio of flow per gram of tissue, is approximately four times greater than to the kidney cortex and 37 times greater than the blood flow to the central nervous system (CNS). Using magnetic resonance imaging (MRI) techniques in normal rats, Nair et al.[2] demonstrated that the ratio of choroidal blood volume is approximately 10 times greater than the blood flow to the retinal circulation. Thus, the choroid represents a thin, highly vascular tissue that is critical for outer retinal function, specifically photoreceptor support.[3]

Anatomically, the choroid has varying caliber vessels. The inner most layer is made up of Bruch's membrane and choriocapillaris. Next, the larger choroidal arteries and veins are located between the choriocapillaris and sclera.[4] The choroid is separated from the sclera by a potential space referred to as the suprachoroidal space (SCS). This space may expand in cases of suprachoroidal effusions and hemorrhages or also may have an advantageous role for intraocular drug delivery.[5]

There are indications to address the choroid surgically. Thus, a better understanding of the biomechanical properties of this tissue is warranted. Performing a chorioretinal biopsy is an uncommon, yet necessary diagnostic procedure that is required in select cases of infiltrative or infectious uveitis of unknown etiology.[6,7] Systemic disorders that affect the uveal tract are numerous and commonly involve neoplastic, infectious, or inflammatory etiologies.[8] In a proposed, yet controversial treatment for end-stage age-related macular degeneration (AMD), several investigators report varying levels of success using a surgical incision to create a choroid–Bruch's–retinal pigment epithelial (CBR) graft that is translocated to the submacular space.[9–13] Also, tumors may be excised surgically with removal of a portion of the choroid.[14–16]

The local, ex vivo biomechanical environment of the sclera[17] and elastic modulus of the iris[18] have been studied in some detail. Elasticity in biologic tissues is critical for the function of various tissues and is defined as the ability to deform reversibly without loss of energy (i.e., stretchiness).[19] There is strong evidence that elasticity in biologic tissues decreases with age.[20]

We hypothesized that choroidal tissue contracts when subjected to a full-thickness, sharp surgical incision. Furthermore, we hypothesized that the extent of tissue contraction inversely correlated with age. We studied tissue contraction of the choroid in pig and human eyes. The rationale for adding pig eyes to this analysis is the ready availability of porcine tissue, the similarity to human eyes, and the ability to study a greater number of surgical variables.

Methods

Tissue was obtained from a local slaughterhouse, and 48 porcine globes from 24 pigs were studied ex vivo and 97 separate incisions were created. Ten human eyes were obtained from the Lions Eye Institute for Transplant and Research (LEITR) in Tampa Bay, Florida. Each pair originated from a donor that died in distinct decades of life (ages 31, 59, 65, 76, or 85 years). A total of 15 incisions were created in these 10 globes. Studies were conducted in compliance with the ARVO Statement for Use of Animals in Ophthalmic and Vision Research. Use of human tissue was designated as exempt status from the Emory Institutional Review Board (IRB) and studies were conducted in accordance with the Declaration of Helsinki for human subjects in research.

All eyes were shipped to the laboratory on ice, in saline moistened containers, within 24 hours from time of death for immediate study. Globes were maintained from 1.7° to 4.4°C before dissection and were discarded once they were more than 24 hours from time of death.

All eyes (pig and human) were transected in a coronal plane using a razor blade and curved scissors to remove the anterior segment. The vitreous was removed. A micro-forceps and curved scissors were used to remove the neurosensory retina gently. Tissues were gently rinsed with balanced salt solution (BSS) to remove debris.

Pig Eyes Procedures

Temperature (Table 1)

Pig eyes were shipped on ice and divided into 2 testing temperature groups. Group A remained at 1.7° to 4.4°C during the dissection. Group B ($n = 16$) eyes were placed in a saline filled bag and warmed to 36.7°C over a period of 1 to 2 hours in a water bath.

Incision

Circular trephines (PSS World Medical, Inc., Jacksonville, FL) were used to create three circular incisions in each pig globe (Fig. 1). Three trephinations were created in each globe (Fig. 2). Trephine diameters were either 1.5, 2.0, or 2.5 mm. Care was taken to maintain the curvilinear anatomy of the sclera–choroid (as opposed to flat mount techniques). Also, care was taken to avoid close contact with the vortex ampullae, optic nerve, or macular region, all representing areas of tight adhesions of the choroid to the sclera. All incisions were full-thickness and extended through the CBR complex, yet not through the sclera. During one of three trephinations in each globe, a blunt spatulated instrument was inserted into the SCS and used to separate or undermine the choroid (Table 1) by breaking any the connective tissue or fibrils within this space. The SCS dissection extended no more than 2.5 mm beyond the trephination.

Table 1. Pig Eyes with Circular Trephine Incision

Variable		Pig Choroid Contraction Area, mm^2			Percent Contraction, %[b]	
Trephine Diameter, mm	Undermining[a] + or −	Group A/C 1.7–4.4°C Temp, $n = 48$	Group B 36.7°C Temp, $n = 49$	Mean, ± SD	Inner Circle	Outer Circle
1.5	−	1.20 ± 0.35	1.34 ± 0.32	1.37 ± 0.36	38*	15*
1.5	+	1.51 ± 0.40	1.37 ± 0.38		46†	14†
2.0	−	2.10 ± 0.35	1.96 ± 0.51	2.18 ± 0.44	38*	18*
2.0	+	2.25 ± 0.52	2.34 ± 0.41		48†	15†
2.5	−	2.94 ± 0.51	3.37 ± 1.19	3.43 ± 0.83	44†	11†
2.5	+	3.92 ± 0.79	3.54 ± 0.57		50‡	15‡
Mean					44‡	15‡

[a] The undermining technique (+) indicates that it was performed, and (–) indicates that it was not performed. The technique uses a blunt spatula for blunt dissection within the suprachoroidal space.

[b] Percent contraction is relative to the true size of the trephine as a ratio of area from the tissue as it contracts either centrifugally (outer circle) or centripetally (inner circle) from the circular incision. n = the total number of trephinations in the column, rather than the number of globes. Group A was processed at 35° to 40°F and group B at 98°F.

* $P < 0.05$, † $P < 0.01$, or ‡ $P < 0.001$ designate significance of the comparison in the percentage contraction from inner to outer circles.

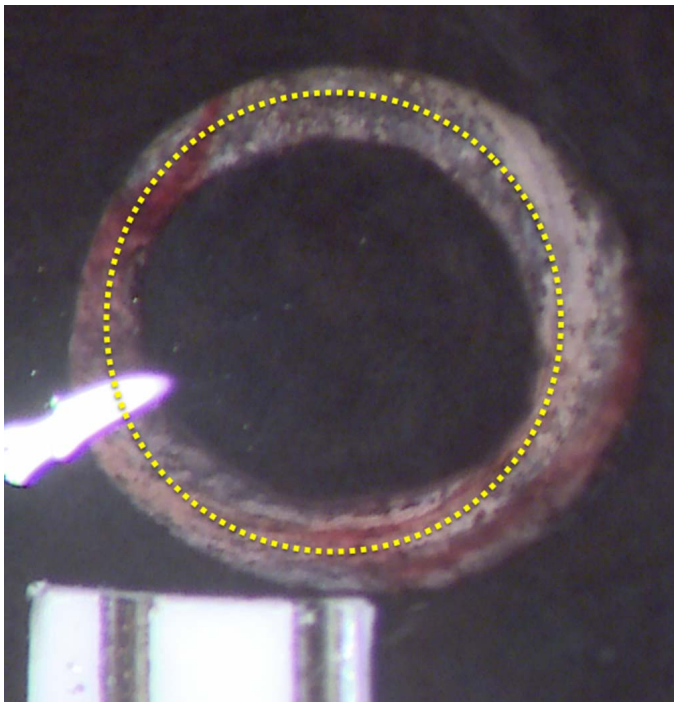

Figure 1. A posttrephination, circular incision through the full-thickness CBR using a 2-mm trephine. The contraction of the tissue is highlighted by the *white*, underlying scleral tissue. The RPE layer is visible at the cut edge. The *dashed yellow line* indicates the trephination zone.

In all group C eyes, a sharp surgical blade (crescent-style) was used to create a linear incision after flat-mounting the sclera and choroid as a unit into a metal clamp (Fig. 3, $n = 16$). The clamp was released, and the globe retained a natural, curvilinear configuration for photography and measurements (Figs. 4A–D).

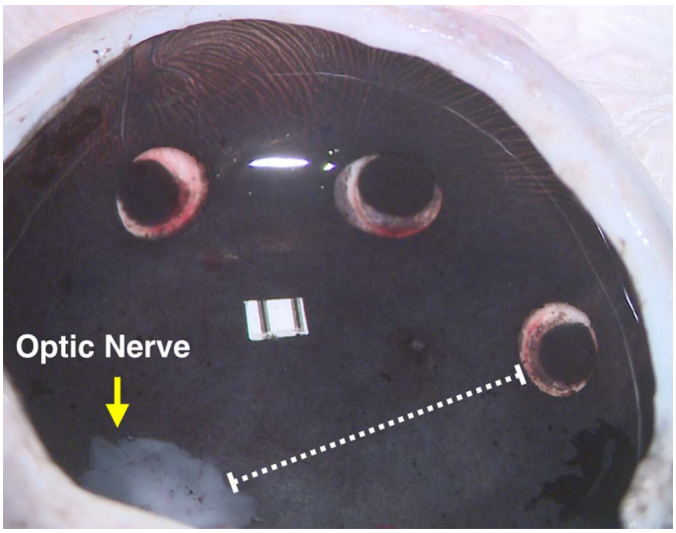

Figure 2. Example of the number of samples or trephinations per globe (average was three). The *dashed line* represents the distance of the posterior most extent of the trephination to the edge of the optic nerve. A reference ruler for measurement is present in the center of the field.

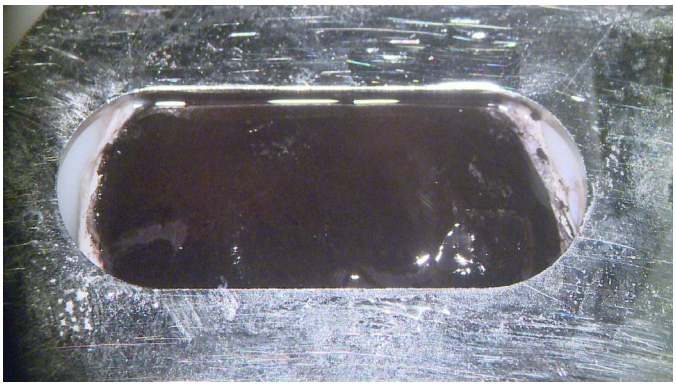

Figure 3. Porcine choroidal tissue and sclera together placed in a linear metal clamp with the dark choroid and RPE on the surface. The linear incision is made parallel to the longest diameter of the clamp. The clamp then is removed quickly and the contraction measured with a calibrated ruler.

Imaging

Following the choroidal incision or trephination, all tissue specimens were photographed immediately with a measuring ruler using a surgical microscope (Zeiss Universal S3 Opmi-6SFC; Oberkochen, Germany) and a digital camera (Exmor Full HD PMW-10MD, Sony Corp., Tokyo, Japan). Alternatively, images were grabbed from video capture. Each measuring ruler was calibrated using an engineering caliper (General Tools and Instruments LLC, Montreal, Canada).

Image Analysis

Images were imported into a computer software program (ImageJ; National Institutes of Health, Bethesda, MD), and the software calculated tissue contraction. In trephination, the borders of the posttrephination tissue on the images were traced and the area of contraction (between the borders) was calculated (mm^2). The ratio of centrifugal contraction of the outer circle tissue-border relative to the trephine incision diameter was used to generate ratio of tissue contraction for the outer circle. Similarly, the ratio of centripetal contraction of the inner circle tissue-border relative to the trephination incision was used to generate a ratio contraction for the inner circle. Ratios were converted to percentages. For the linear incisions (Fig. 5), a simple linear postincision measurement was taken of the incision length and maximum width (contraction). Figure 5 describes the geometry of measurements taken for circular and linear incisions.

For the circular trephination incisions, the degree of asymmetry for each incision was determined using the aspect ratio or the ratio of irregularities along the incision (Fig. 6). Computer software tracing calculates the actual area of contraction from manually traced outlines at the edge of the tissue border. The aspect ratio was quantified from 0.0 (very irregular) to 1.0 (perfectly round).

Human Eyes (n = 10 Globes from 5 Donors)

Globes were procured from varying age eye bank donors procured from LEITR. Age at death for the donors was 31, 59, 65, 76, and 85 years. Globes were processed as described above and each CBR incision was made using a 2-mm diameter trephine (Table 2)

Statistical Analysis

A 2-tailed Student *t*-test was used to determine significance between the mean group measurement ratios (± standard deviation [SD]). Linear regression analysis was used to determine the relationship between linear incision length and the width of contraction or donor age and contraction.

Results

Pig Eye Trephination (Group A and B)

The area of contraction for each group (A and B) are listed in Table 1. Temperature variation was minimal. The centripetal contraction area increased with increasing size of trephine diameter ($P < 0.001$). The centripetal contraction was significantly greater than the area of centrifugal outer circle outward contraction ($P < 0.05$) using the 1.5 mm trephine (Table 1). For comparison of the centripetal:centrifugal contraction area, the 2.0 and 2.5 mm trephines showed a statistical difference ($P < 0.01$ and $P < 0.001$, respectively). Interestingly, the area of centrifugal contraction did not change from the 1.5, 2.0, or 2.5 mm incisions ($P = 0.45$).

Suprachoroidal Disinsertion

Blunt dissection of the suprachoroidal adventitia resulted in a meaningful and statistically significant increase of inner centripetal ($P < 0.001$) and outer centrifugal ($P < 0.001$) and combined or total choroidal tissue contraction ratio ($P < 0.001$) at all temperatures (Figs. 7–9). However, compared to choroid with intact adventitia, disinsertion of the suprachoroidal adventitia displayed a more exaggerated centripetal tissue contraction, ($P < 0.01$) than external centrifugal contraction at both temperatures, $P < 0.001$ (Figs. 7–9).

Figure 4. Porcine tissue, sclera, CBR clamped in a flat mount clamp for incision with a crescent-style surgical blade. (A) Clamped tissue pre-incision. (B) Active incision. (C) Incision with clamp removed and a measuring device for length of incision. (D) Measurement of incision width.

Distance from the Optic Nerve

By comparing the same trephination to the measured distance of the posterior edge of the trephination to the optic nerve, there was a weak correlation that was not meaningful.

Aspect Ratio

The relative symmetry or asymmetry of the choroidal contraction measurements following trephination was determined to be consistently similar within the varying size of trephination as well as across both temperatures. Measurements of the mean aspect ratios were highly variable within groups, yet there were no significant differences or relevant changes between groups. Asymmetry likely represents the ability of the trephine to incise the tissue sharply without leaving irregular edges. Thus, while there were irregularities, there were no significant differences between groups.

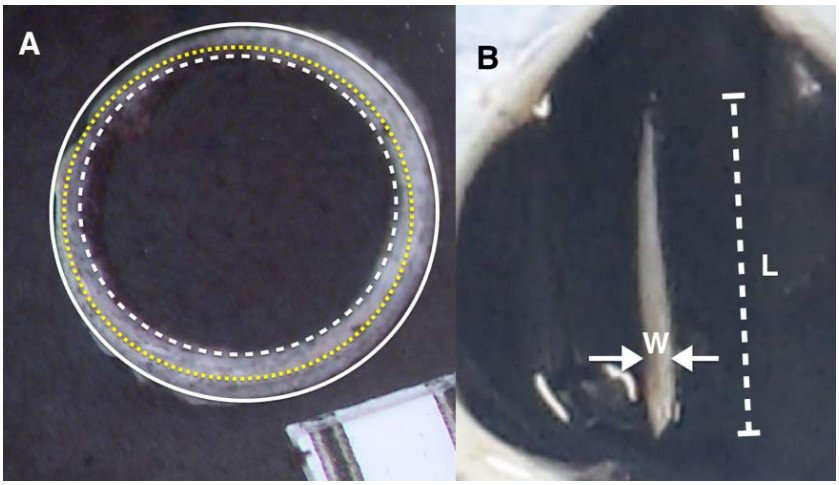

Figure 5. (A) Schematic of the linear and trephination of the tissue. Linear measures are in millimeters. The center ring (*small yellow dots*) represents the trephine cut. The inner circle (*dashed white line*) is the inner circle centripetal contraction and the area between these *two circles* is the inner circle contraction (mm^2). The *outer circle* (*solid white line*) represents the outer circle centrifugal contraction as measured from the *center ring* (*small yellow dots*). The total contraction is the sum of these two areas. (B) The linear incisions (L) length is measured from the apices of the incision (*dashed white line*; mm) and the width (W) is the greatest perpendicular measurement (mm).

Linear Incision; Group C ($n = 16$)

The contraction of the choroid, relative to the linear incision (Group C), was measured at the greatest perpendicular separation between tissue edges (90° from the incision). Figure 10 represents the linear relationship between the length of the linear, sharp incision and the perpendicular length of incision contraction in millimeters ($R^2 = 0.02$, $R = 0.14$, $P \leq 0.001$). This ratio suggested that the degree of maximum perpendicular contraction is predictable and depends upon the length of the linear incision.

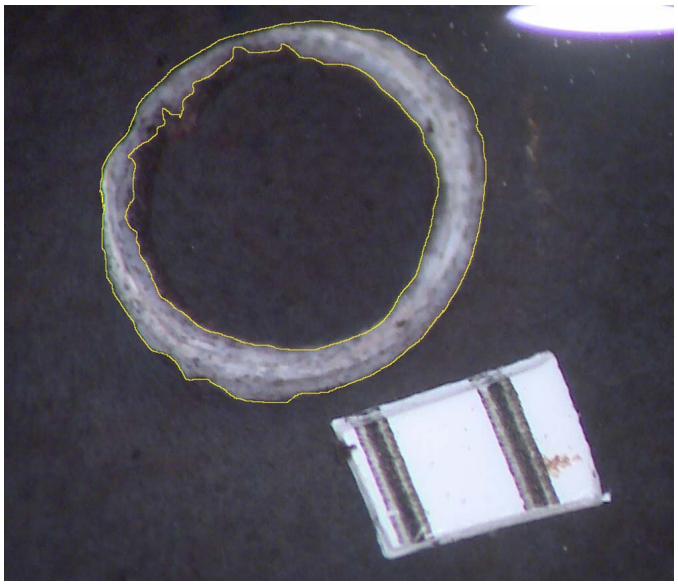

Figure 6. Computer software tracing calculates the actual area of contraction from manually traced outlines at the edge of the tissue border. The aspect ratio varies from 0.0 to 1.0 or a perfectly consistent border. The aspect ratio in image is 0.83 (note the irregularities and some asymmetry).

Human Globes (Table 2)

Choroidal contraction was similar to the contraction seen with pig eyes. The data were similar for each decade assessed. Using three, 2.0 mm trephinations per globe, six measurements were obtained from each donor for a total of 30 measurements (Fig. 11). Only the 85-year-old donor had a relevant decrease in the area of contraction (Fig. 12). The cause of death in this individual was cardiovascular disease, a particularly common etiology in this age group. By examining the linear regression analysis, there was a statistically significant inverse relationship of age and choroidal contraction ($R^2 = 0.35$, $P < 0.001$; Fig. 13). As seen with the pigs, the inner circle, centripetal contraction measurements were greater than the outer circle, centrifugal contractions ($P < 0.001$). Furthermore, when the SCS was undermined with blunt dissection, there was an increase in the centripetal choroidal contraction measurements (inner contraction), greater than the outer circle, centrifugal contraction measurements ($P < 0.001$; Fig. 11). Finally, the total choroidal tissue contraction measured area was greater when the SCS was undermined

Table 2. Human Eyes with Circular Trephine Incision

Variable		Human Choroid Contraction Area, mm^2			Percent Contraction, %[b]	
Trephine Diameter, mm	Undermining[a] + or −	Group A 1.7–4.4°C Temp	Group B 36.7° C Temp, $n = 15$	MEAN, ± SD	Inner Circle	Outer Circle
2.0	–	N/A	1.76 ± 0.39	1.93 ± 0.41	38	11
2.0	+	N/A	2.10 ± 0.38		40	19
Mean					39	15

[a] The undermining technique (+) indicates that it was performed, and (–) indicates that it was not performed. The technique uses a blunt spatula blunt separation within the suprachoroidal space.

[b] Percent contraction is relative to the true size of the trephine as a ratio of area from the tissue as it contracts either centrifugally (outer circle) or centripetally (inner circle) from the circular incision. n = the total number of trephination in the column, rather than the number of globes.

compared to eyes where the SCS was undisturbed ($P \leq 0.05$; Fig. 11).

Discussion

Choroidal surgery, as with all forms of invasive surgery, involves creating a full-thickness surgical incision. Approaching the choroid surgically, a unique and highly specialized multilaminar tissue, warrants extreme caution and further study is needed to create the best possible environment for such an incision. The vascular nature of the choroid represents a high-risk surgical environment for any elective surgical incision. Hemostasis during a choroidal incision is paramount and extremely challenging, especially given that this tissue has the highest measured blood flow per gram of tissue in the body.[1] A suprachoroidal hemorrhage may lead to severe complications and even blindness.[21–23] The choroidal vascular anatomy[24] has numerous anastomotic chan-

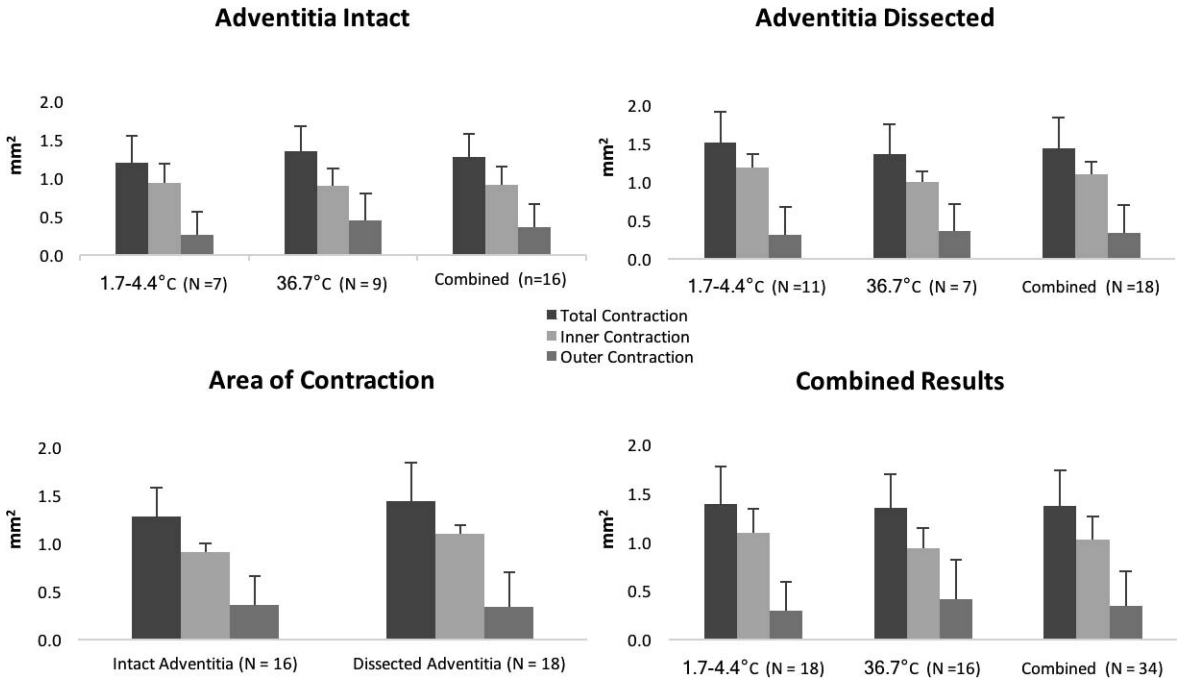

Figure 7. Area of tissue contraction from a full-thickness choroidal incision using a 1.5 mm trephines on porcine globes. *Bar graphs* compare total area of contraction (*dark gray bars*) that is the sum of the inner centripetal (*light gray*) and the outer centrifugal (*medium gray*) contraction area. The significance of the comparison in the percentage contraction using *$P < 0.05$, †$P < 0.01$, or ‡$P < 0.001$.

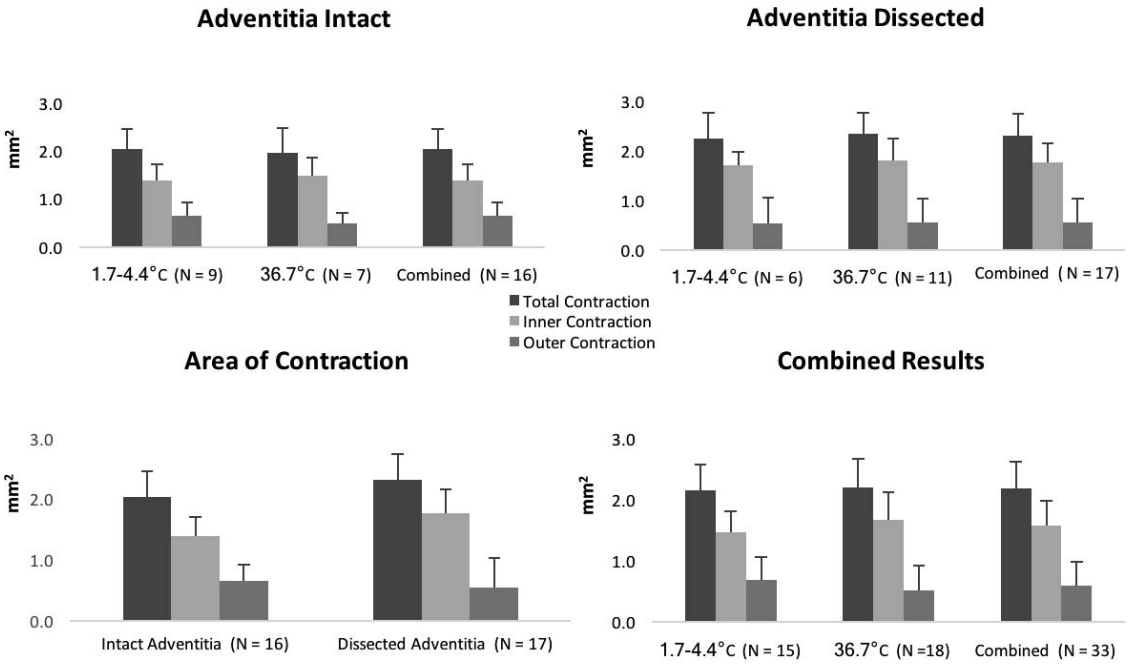

Figure 8. Area of tissue contraction from a full-thickness choroidal incision using a 2.0 mm trephines on porcine globes. *Bar graphs* compare total area of contraction (*dark gray bars*) that is the sum of the inner centripetal (*light gray*) and the outer centrifugal (*medium gray*) contraction area. The significance of the comparison in the percentage contraction using $*P < 0.05$, $\dagger P < 0.01$, or $\ddagger P < 0.001$.

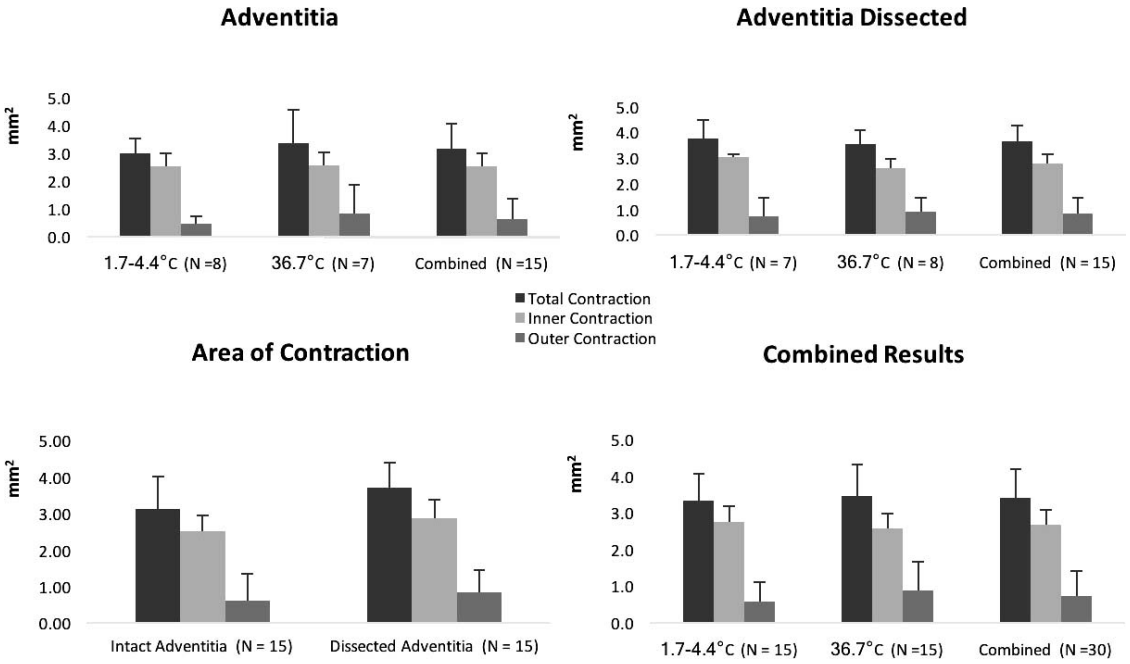

Figure 9. Area of tissue contraction from a full-thickness choroidal incision using 2.5 mm trephines on porcine globes. *Bar graphs* compare total area of contraction (*dark gray bars*) that is the sum of the inner centripetal (*light gray*) and the outer centrifugal (*medium gray*) contraction area. The significance of the comparison in the percentage contraction using $*P < 0.05$, $\dagger P < 0.01$, or $\ddagger P < 0.001$.

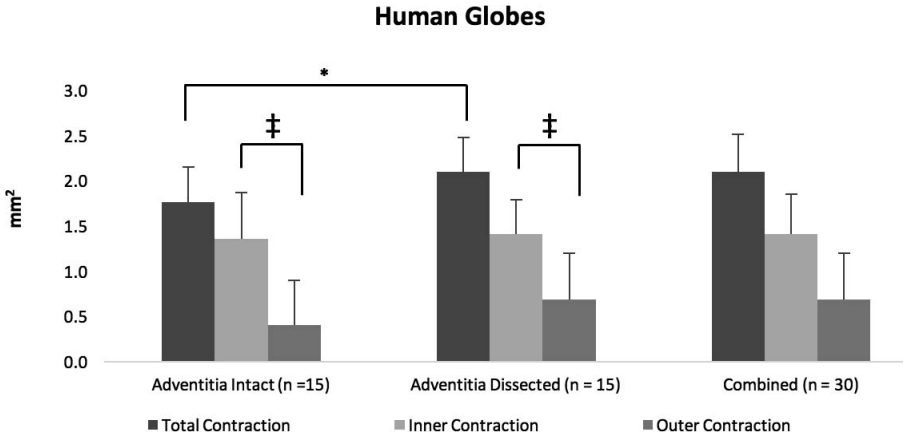

Figure 10. Area of tissue contraction from a full-thickness choroidal incision with 2.0 mm trephines on human globes. Internal contraction was significantly greater than external contraction for intact, dissected, and combined adventitia. Significance is listed at $*P < 0.05$, $\dagger P < 0.01$, or $\ddagger P < 0.001$.

nels and, thus, closure of vessels during an intervention, incision, or injury usually leads to redirection of blood flow and normalization of perfusion. Since this was an ex vivo study, we obviously cannot assess hemostasis. Instead, we have chosen to document the biomechanical response ex vivo. In prior in vivo studies, we documented a rapid vascular redirection and normalization of choroidal perfusion when studying blood flow in the primate model relative to an injury from a suprachoroidal drug delivery cannulae.[5] Thus, such a rich anastomotic environment may serve to redirect and reperfuse choroidal flow following an incision or injury. Further in vivo studies are warranted to understand this capacity better.

During ophthalmic surgery, especially in cases of trauma or when choroidal tissue is biopsied for diagnostic purposes, contraction of the surrounding choroidal tissue is readily apparent to the surgeon. To the best of our knowledge, documentation or measurements of this contraction have not been studied to date. During a full-thickness, traumatic injury to the choroid, such as in traumatic chorioretinal rupture or sclopetaria,[25] there typically is a relatively large, retracted choroidal wound edge, creating a rather large, clinically-relevant residual defect. Also, during an elective chorioretinal biopsy (either incisional or excisional), frequently performed for diagnostic purposes, two observations are consistent. First, the ex vivo biopsy specimen size is smaller than the surgeon's demarcated biopsy area. This corresponds to the inner circle centripetal contraction measured in this study. Second, the size of the residual defect at the biopsy site is larger than the surgeon's

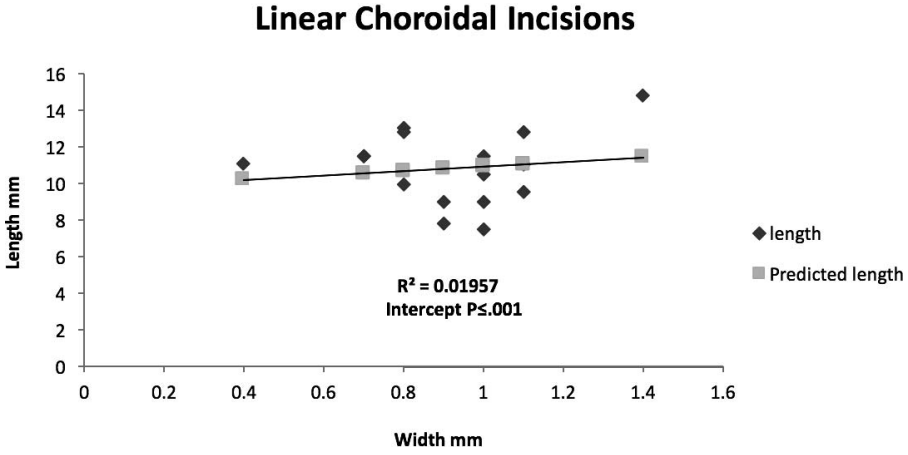

Figure 11. Linear graph comparing the length of the incision to the perpendicular length of contraction. There is a direct correlation between length of incision and choroidal contraction ($R^2 = 0.0196$, $R = 0.14$; intercept $P \leq 0.001$).

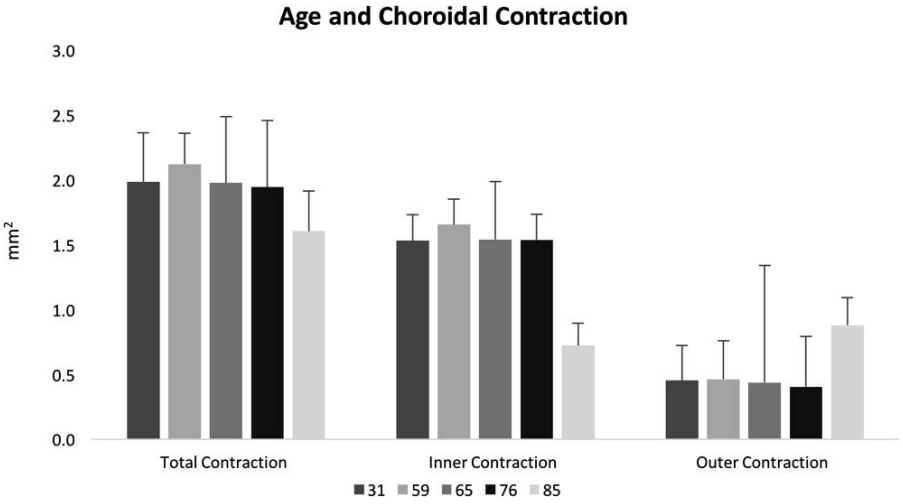

Figure 12. Area of choroidal contraction area of human globes by age.

demarcated biopsy area. This corresponds to the outer circle centrifugal contraction, similarly measured in this study.

Our ex vivo model allows us to study the variables that may affect tissue elasticity and contraction. In the ex vivo environment, we controlled for tissue temperature. Thus, Groups A to C were monitored at different temperatures. While minor differences related to temperature were noted, these were not felt to contribute in a meaningful way to the results of our measurements. All of the tissues (porcine and human) were fresh, placed on ice after enucleation, and used immediately postmortem rather than being subjected to freezing. We believed that, while there may well have been some autolytic enzymatic activity, our goal was to minimize temperature as a postmortem variable. All porcine and human eyes were processed within 24 hours from the time of death. Temperature, water, acidity, and availability of oxygen can moderate the internal chemical and biological progression of postmortem tissue decomposition.[26] Since all specimens were relatively fresh and handled similarly, we anticipated that each group of data acquired was similarly affected by these postmortem tissue conditions.

In surgical incisions, either trephination or blade incision, the choroid retracts away from an incision. For a linear incision, the maximum retraction or separation of the tissues has a significant and positive correlation with the length of the incision (Figs. 4, 10).

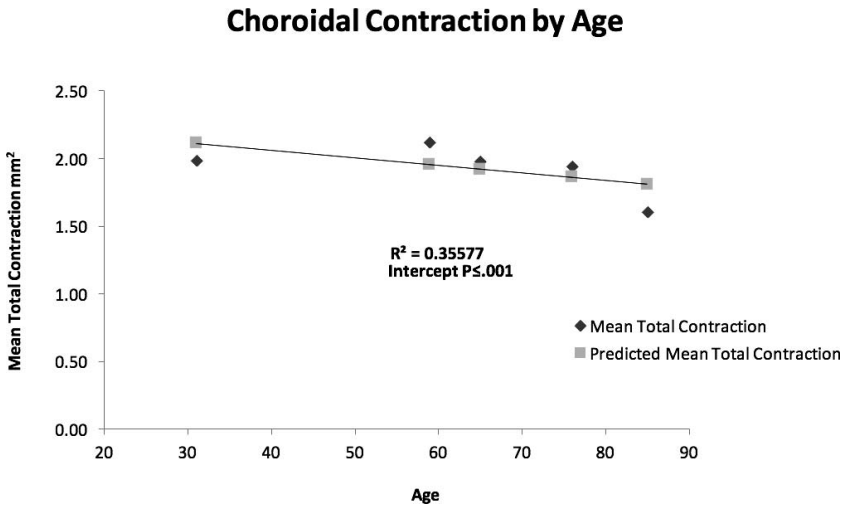

Figure 13. Linear graph comparing contraction of the trephined choroidal tissue with donor age. There is a direct correlation between length of incision and choroidal contraction ($R^2 = 0.35$, $R = -0.59$; $P < 0.001$).

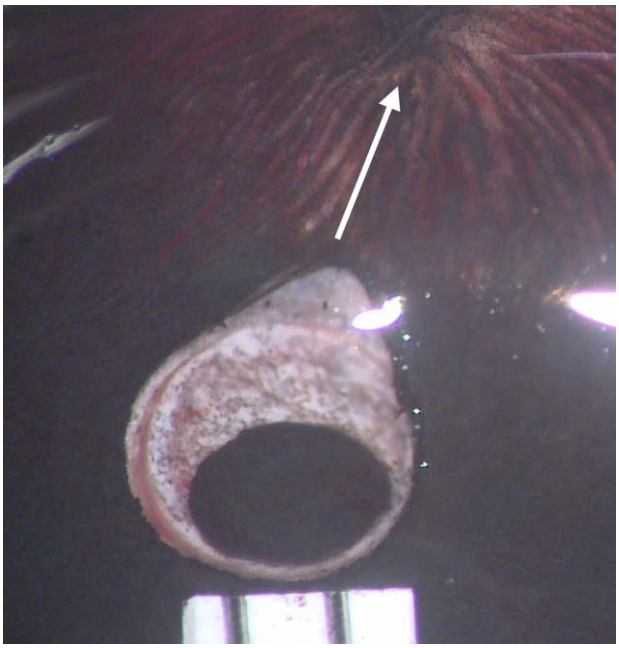

Figure 14. The retraction asymmetry of the outer circle centrifugal pattern (see *arrow*) is toward the vortex ampullae.

Such a proportional retraction from a linear incision is expected in any elastic tissue.[27,28] Indeed, the highly vascular architecture of the choroid contributes to its elasticity and contraction as has been documented in other vascular systems.[29,30] Thus, a choroidal incision may contract from elastin found in Bruch's membrane and the elastin and smooth muscle found in choroidal vessels. Other studies have documented arterial retraction upon transection in human and animal models.[29,31] External iliac arteries in human cadavers retracted approximately 15% following an incision.[32] The concept, described as postincisional arterial contraction, has been described in terms of axial prestretch and suggests that there is a defined length that tissues are stretched during development.[33] Axial prestretch also is referred to as longitudinal traction and has a linear correlation with postnatal development. During postnatal development, more contraction of the carotid arteries occurs as the elastic laminae stretches and the vessel grows in diameter during maturation.[31] In our model, we believe that Bruch's membrane and the choroidal vasculature both contribute to postincisional choroidal contraction. Vascular contributions to the elastic forces result from unloaded axial prestretch as well as longitudinal traction.

Another important variable that determines the extent of postincisional choroidal contraction is the status of the choroidal-scleral connections. The tight adhesions anatomically occur at the optic nerve, short, posterior ciliary arteries near the macula, the vortex ampullae, and at the scleral spur. We avoided these areas as much as possible and did not find a correlation of contraction to distance of the incision from the optic nerve. Contraction patterns seemed to be influenced by the vortex ampullae (Fig. 14). In this image, there is a teardrop outer circle contraction that points toward the visible vortex ampullae. Thus, we suspect that the closer an incision is to the tight adhesion, the greater the directional contraction. While the distance from the optic nerve was not found to be an important variable for contraction, we intentionally avoided incisions close to the optic nerve (Fig. 2). Thus, while there may be a similar asymmetric contraction as was seen relative to the vortex ampullae, we did not fully investigate this relationship to the optic nerve or macula. Yet another variable that we did not consider in this analysis is the degree of myopia and axial length. One may hypothesize that myopic eyes with a greater axial length may have even greater tissue contraction. The lens status of the eye also may influence contraction, but to a lesser degree. These latter two variables were not analyzed in this study, yet remain as influential variables.

Weak, fibrous connections exist between the choroid and sclera in zones between the tight adhesions that have been documented using endoscopy in a primate model.[5] Such adhesions do not seem to create a barrier to suprachoroidal drug delivery.[5,34] In our studies, some trephinations were pretreated using a spatula to dissect these small, fibrous adhesions bluntly. Indeed, we found that there were increasing choroidal contraction measurements, likely due to less subjacent adhesion or anchoring of the underlying sclera when these connections were interrupted. The best demonstration of this contraction is represented by the 50% inner circle centripetal contraction that was documented using the larger 2.5 mm trephine (Table 1). By contrast, the 38% inner circle centripetal contraction measure was much lower using the 1.5 mm trephination. Within each increase in trephination size, there was a significantly greater contraction ratio when suprachoroidal adhesions were interrupted than when they remained intact. In an eye that has had a prior suprachoroidal effusion or detachment, the choroid may be particularly susceptible to contraction should a choroidal incision be required (i.e., for a choroidal biopsy).

In human and porcine globes, the direction of

inner circle centripetal contraction accounted for the majority of the tissue contraction. This may be due to complex geometry and the physical force vectors. Inner centripetal contraction may alleviate most of the stored elastic tension within the tissue. In models that study the boundaries of gel contractions, asymmetric contraction occurs along a curvilinear boundary line due to an imbalance of tangential forces.[35] Detailed analysis of the elastic modulus (Young's modulus) for an anisotropic tissue, such as the choroid, with nonlinear forces is beyond the scope of this study, yet such an approach may lead to a better understanding of our observations.

In human eyes, we observed the same trends that were documented in pig eyes (Tables 1, 2), thus, confirming that the pig model is a reliable model with application to humans. We specifically requested human globes from differing decades so that we could determine if there is a change in choroidal contraction that corresponds to advancing age. Indeed, we found a statistically significant negative correlation. Not surprisingly, the choroidal tissue seems to become less elastic or stiffer with age. This may be due to crosslinking of collagen tissues as occurs in the cornea.[36] The oldest human subject (85 years old) had particularly low tissue contraction areas. This may have been due to aging or an underlying systemic disorder that was not reported in the limited medical history obtained. A larger study with more subjects of varying age would help to better define the variables.

In summary, we demonstrated, measured, and confirmed the ex vivo contraction of the choroid when subject to linear and circular incisions in pig and human eyes. We controlled variables, such as time postmortem, temperature, undermining, incision size, and location relative to the optic nerve and vortex ampullae. A circular incision or trephination leads to contraction of tissue away from the incision circumference. The linear incision contraction is perpendicular and corresponds directly to the incision length. For a circular incision, there is a greater degree of centripetal contraction within the inner circle than the centrifugal outer circular contraction. By undermining and breaking the loose adhesions between the choroid and sclera, within the suprachoroidal space, we measured a statistically significant increase in tissue contraction, particularly for larger incisions and for the centripetal inner circle contraction. This has clinical relevance for chorioretinal biopsies, tumor excisions, and also for macular translocation surgery. Finally, we measured an inverse correlation of choroidal tissue contraction and age. Finally, our hypothesis is confirmed and the elasticity in the choroid leads to postincisional tissue contraction. Furthermore, these measurements have been quantified relative to key, predetermined variables.

Acknowledgements

The authors thank the Lions Eye Institute for Transplant and Research (LEITR) in Tampa Bay, FL, who provided the tissue.

Supported by the R. Howard Dobbs Jr. Foundation, the Lions Eye Institute for Transplantation and Research, an unrestricted grant from Research to Prevent Blindness (RPB), and the Retina Research Foundation of California.

Disclosure: **S.A. LoBue**, None; **N. Yamada**, None; **M.J. Choi**, None; **T.W. Olsen**, founder of iMacular Regeneration, LLC, no technology discussed in this manuscript is related to that of iMacular Regeneration, LLC

References

1. Alm A, Bill A. The oxygen supply to the retina. II. Effects of high intraocular pressure and of increased arterial carbon dioxide tension on uveal and retinal blood flow in cats. A study with radioactively labelled microspheres including flow determinations in brain and some other tissues. *Acta Physiol Scand*. 1972;84:306–319.
2. Nair G, Tanaka Y, Kim M, et al. MRI reveals differential regulation of retinal and choroidal blood volumes in rat retina. *Neuroimage*. 2011;54:1063–1069.
3. Nickla DL, Wallman J. The multifunctional choroid. *Prog Retin Eye Res*. 2010;29:144–168.
4. Spraul CW, Lang GE, Grossniklaus HE. Morphometric analysis of the choroid, Bruch's membrane, and retinal pigment epithelium in eyes with age-related macular degeneration. *Invest Ophthalmol Vis Sci*. 1996;37:2724–2735.
5. Olsen TW, Feng X, Wabner K, et al. Cannulation of the suprachoroidal space: a novel drug delivery methodology to the posterior segment. *Am J Ophthalmol*. 2006;142:777–787.

6. Cheng NM, Chandra A, Roufail E, et al. Chorioretinal biopsy for the diagnosis of endogenous endophthalmitis due to Escherichia coli. *Retin Cases Brief Rep*. 2017;11:30–33.
7. Cole CJ, Kwan AS, Laidlaw DA, Aylward GW. A new technique of combined retinal and choroidal biopsy. *Br J Ophthalmol*. 2008;92: 1357–1360.
8. Olsen TW, Palejwala NV, Lee LB, Bergstrom CS, Yeh S. Chorioretinal folds: associated disorders and a related maculopathy. *Am J Ophthalmol*. 2014;157:1038–1047.
9. Lu Y, Han L, Wang C, et al. A comparison of autologous transplantation of retinal pigment epithelium (RPE) monolayer sheet graft with RPE-Bruch's membrane complex graft in neovascular age-related macular degeneration. *Acta Ophthalmol*. 2016;95:e443–e452.
10. van Zeeburg EJ, Cereda MG, Amarakoon S, van Meurs JC. Prospective, randomized intervention study comparing retinal pigment epithelium-choroid graft surgery and Anti-VEGF therapy in patients with exudative age-related macular degeneration. *Ophthalmologica*. 2015;233:134–145.
11. van Zeeburg EJ, Maaijwee KJ, Missotten TO, Heimann H, van Meurs JC. A free retinal pigment epithelium-choroid graft in patients with exudative age-related macular degeneration: results up to 7 years. *Am J Ophthalmol*. 2012;153: 120–127 e122.
12. Maaijwee K, Joussen AM, Kirchhof B, van Meurs JC. Retinal pigment epithelium (RPE)-choroid graft translocation in the treatment of an RPE tear: preliminary results. *Br J Ophthalmol*. 2008;92:526–529.
13. Heussen FM, Fawzy NF, Joeres S, et al. Autologous translocation of the choroid and RPE in age-related macular degeneration: 1-year follow-up in 30 patients and recommendations for patient selection. *Eye (Lond)*. 2008;22:799–807.
14. Peyman GA, Gremillion CM. Eye wall resection in the management of uveal neoplasms. *Jpn J Ophthalmol*. 1989;33:458–471.
15. Peyman GA, Apple DJ. Local excision of choroidal malignant melanoma. *Arch Ophthalmol*. 1974;92:216–218.
16. Foulds WS. The local excision of choroidal melanomata. *Trans Ophthalmol Soc U K*. 1973; 93:343–346.
17. Wang R, Raykin J, Gleason RL Jr, Ethier CR. Residual deformations in ocular tissues. *J R Soc Interface*. 2015;12.
18. Whitcomb JE, Barnett VA, Olsen TW, Barocas VH. Ex vivo porcine iris stiffening due to drug stimulation. *Exp Eye Res*. 2009;89:456–461.
19. Gosline J, Lillie M, Carrington E, Guerette P, Ortlepp C, Savage K. Elastic proteins: biological roles and mechanical properties. *Philos Trans R Soc Lond B Biol Sci*. 2002;357:121–132.
20. Sherratt MJ. Tissue elasticity and the ageing elastic fibre. *Age (Dordr)*. 2009;31:305–325.
21. Goldsmith C, Rene C. Massive spontaneous expulsive suprachoroidal haemorrhage in a blind glaucomatous eye treated with chronic topical steroid. *Eye (Lond)*. 2003;17:439–440.
22. Stein JD, Zacks DN, Grossman D, Grabe H, Johnson MW, Sloan FA. Adverse events after pars plana vitrectomy among medicare beneficiaries. *Arch Ophthalmol*. 2009;127:1656–1663.
23. Garrott HM, Haynes RJ. Blindness from suprachoroidal haemorrhage in two patients with age-related macular degeneration on systemic anticoagulation therapy or an antiplatelet agent. *Med J Aust*. 2010;192:346–347.
24. Weiter JJ, Ernest JT. Anatomy of the choroidal vasculature. *Am J Ophthalmol*. 1974;78:583–590.
25. Martin DF, Awh CC, McCuen BW II, Jaffe GJ, Slott JH, Machemer R. Treatment and pathogenesis of traumatic chorioretinal rupture (sclopetaria). *Am J Ophthalmol*. 1994;117:190–200.
26. Campobasso CP, Di Vella G, Introna F. Factors affecting decomposition and Diptera colonization. *Forensic Sci Int*. 2001;120:18–27.
27. Essner E, Gordon SR. Demonstration of microfibrils in Bruch's membrane of the eye. *Tissue Cell*. 1984;16:779–788.
28. Newsome DA, Huh W, Green WR. Bruch's membrane age-related changes vary by region. *Curr Eye Res*. 1987;6:1211–1221.
29. Dobrin P, Canfield T. Identification of smooth muscle series elastic component in intact carotid artery. *Am J Physiol*. 1977;232:H122–130.
30. Karimi A, Milewicz DM. Structure of the elastin-contractile units in the thoracic aorta and how genes that cause thoracic aortic aneurysms and dissections disrupt this structure. *Can J Cardiol*. 2016;32:26–34.
31. Dobrin P, Canfield T, Sinha S. Development of longitudinal retraction of carotid arteries in neonatal dogs. *Experientia*. 1975;31:1295–1296.
32. Dobrin PB, Schwarcz TH, Mrkvicka R. Longitudinal retractive force in pressurized dog and human arteries. *J Surg Res*. 1990;48:116–120.
33. Cardamone L, Valentin A, Eberth JF, Humphrey JD. Origin of axial prestretch and residual stress

in arteries. *Biomech Model Mechanobiol*. 2009;8: 431–446.
34. Olsen TW, Feng X, Wabner K, Csaky K, Pambuccian S, Cameron JD. Pharmacokinetics of pars plana intravitreal injections versus microcannula suprachoroidal injections of bevacizumab in a porcine model. *Invest Ophthalmol Vis Sci*. 2011;52:4749–4756.
35. Schuppler M, Keber FC, Kroger M, Bausch AR. Boundaries steer the contraction of active gels. *Nat Commun*. 2016;7:13120.
36. Elsheikh A, Wang D, Brown M, Rama P, Campanelli M, Pye D. Assessment of corneal biomechanical properties and their variation with age. *Curr Eye Res*. 2007;32:11–19.